MOLECULAR AND CELLULAR BIOLOGY, Oct. 2004, p. 8408–8417 Vol. 24, No. 19
0270-7306/04/$08.00+0 DOI: 10.1128/MCB.24.19.8408–8417.2004
Copyright © 2004, American Society for Microbiology. All Rights Reserved.

Selective Decrease in Paracellular Conductance of Tight Junctions: Role of the First Extracellular Domain of Claudin-5

Huajie Wen, Debbie D. Watry, M. Cecilia G. Marcondes, and Howard S. Fox*

Department of Neuropharmacology, The Scripps Research Institute, La Jolla, California 92037

Received 3 February 2004/Returned for modification 17 March 2004/Accepted 29 June 2004

Claudin-5 is a protein component of many endothelial tight junctions, including those at the blood-brain barrier, a barrier that limits molecular exchanges between the central nervous system and the circulatory system. To test the contribution of claudin-5 to this barrier function of tight junctions, we expressed murine claudin-5 in Madin-Darby canine kidney II cells. The result was a fivefold increase in transepithelial resistance in claudin-5 transductants and a reduction in conductance of monovalent cations. However, the paracellular flux of neither neutral nor charged monosaccharides was significantly changed in claudin-5 transductants compared to controls. Therefore, expression of claudin-5 selectively decreased the permeability to ions. Additionally, site-directed mutations of particular amino acid residues in the first extracellular domain of claudin-5 altered the properties of the tight junctions formed in response to claudin-5 expression. In particular, the conserved cysteines were crucial: mutation of either cysteine abolishted the ability of claudin-5 to increase transepithelial resistance, and mutation of Cys^{64} strikingly increased the paracellular flux of monosaccharides. These new insights into the functions of claudin-5 at the molecular level in tight junctions may account for some aspects of the blood-brain barrier's selective permeability.

The blood-brain barrier (BBB) is a network of continuous capillaries surrounded by a basal lamina and astrocytic foot processes. Under physiological conditions, the BBB selectively regulates the intracellular and paracellular exchange of macromolecules and cells between the circulation and the central nervous system through several unique structural and functional attributes. Most distinct among these attributes is the presence of high-resistance interendothelial zonulae occludentes, or tight junctions (TJs).

The TJ is an occluding seal between the neighboring cells of an endothelium or epithelium that is located at the most apical part of their lateral membranes. Transmission electron microscopy shows that neighboring plasma membranes make very close contacts, or "kisses," whereas freeze-fracture microscopy reveals that these contacts appear as a series of continuous, anastomosing intramembranous particle strands or fibrils with complementary grooves (51). The paracellular space in the TJ is completely obliterated after each strand associates laterally with a strand in the membrane of an adjacent cell to form "paired" strands (52), generating a primary barrier to the flux of fluid, electrolytes, and macromolecules (2). TJs vary in tightness and permeability between individual cell and tissue types, forming compositionally distinct fluid compartments in multicellular organisms.

In addition to their barrier function, TJ strands permit the paracellular flux of solutes, showing ion and size selectivity that varies significantly in different tissues as specific physiological situations demand. Thereby, the interior environment of each compartment remains uniquely individualized (16, 50).

Retention of the proper structure and function of TJs is essential for maintenance of the BBB (14, 37, 53, 57). Therefore, to understand the mechanisms of BBB function, we examined the roles of its specific components. The first step was to identify a protein expressed at the BBB, known as mouse brain endothelial cell 1 (MBEC1), through a differential RNA expression experiment (8). Based on its homology to the two *Clostridium perfringens* enterotoxin receptors, we proposed that these proteins constitute a distinct family of proteins. These two enterotoxin receptors and MBEC1, indeed, are members of the claudin family of proteins (claudin-3, -4, and -5, respectively), now thought to be the predominant component of TJ strands (1, 52). Among these, claudin-5 was found to be expressed predominantly in endothelial cells, including those at the BBB (8, 41). Thus, in addition to the previously recognized TJ components found at the BBB, such as occludin and ZO-1, claudin-5 may also contribute to BBB TJ function.

The claudins are, in general, closely related to each other but without striking similarity to occludin or to the connexins, four transmembrane domain proteins that make up gap junctions (27). The claudins are predicted to have four transmembrane domains, with a short N terminus, two extracellular domains, and a cytoplasmic tail. A particularly notable feature of the first extracellular domain (ECD) is its regions of conservation as well as diversity. Among the conserved elements are two cysteine residues, located (in claudin-5) at residues 54 and 64. This domain also contains many hydrophobic residues as well as individual charged residues.

To date, about 20 members of the claudin family have been found with varied distribution patterns according to tissue type, which might account for those tissues' different degrees of permeability (20, 31, 45). Claudins polymerize into linear fibrils when expressed in claudin-null fibroblasts, and when occludin is transfected into claudin-expressing fibroblasts, it is recruited into the claudin fibrils (19), suggesting that claudins are the major element driving fibril formation. Accordingly, the depletion or mutation of endogenous claudin or expression

* Corresponding author. Mailing address: Mailstop CVN-1, 10550 North Torrey Pines Rd., La Jolla, CA 92037. Phone: (858) 784-7171. Fax: (858) 784-7296. E-mail: hsfox@scripps.edu.

of exogenous claudin altered both the ion selectivity and permeability of TJs (18, 28, 54).

Within the cell, occludin and claudins interact with the PDZ domains of ZO-1 and ZO-2 (24, 29). ZO-1 and ZO-2 are believed to be involved in creating and maintaining specialized membrane domains by cross-linking multiple integral membrane proteins at the cytoplasmic surface of plasma membranes. ZO-1 and ZO-2 also bind to actin filaments at their C-terminal regions, functioning as a cross-linker between TJ fibrils and the cytoskeleton (17, 26).

In the present studies, expression constructs containing wild-type claudin-5 or claudin-5 mutants were transduced into MDCK II cells, because these cells express occludin, ZO-1, and other necessary protein components of the TJ. We used the first ECD of claudin-5 as the location for introduction of site-directed mutations based on the conservation of particular amino acid residues across the claudin family. The result of claudin-5 expression was a marked increase in transepithelial resistance (TER), and this increase was dependent on the presence of both of the two cysteine residues in the first ECD.

MATERIALS AND METHODS

Antibodies and cell culture. The following commercial antibodies were used in this study: rabbit anti-claudin-1 and anti-occludin polyclonal antibodies and mouse monoclonal anti-claudin-2, anti-claudin-4, anti-claudin-5, and anti-occludin antibodies (Zymed Laboratories, Inc., South San Francisco, Calif.); goat anti-ZO-1 antibody (Santa Cruz Biotechnology, Inc., Santa Cruz, Calif.); rabbit antiactin antibody (Sigma, St. Louis, Mo.); Texas Red-labeled donkey anti-rabbit immunoglobulin G, Texas Red-labeled donkey anti-mouse immunoglobulin G, and fluorescein isothiocyanate-labeled donkey anti-mouse immunoglobulin G (Jackson ImmunoResearch Laboratories, Inc. West Grove, Pa.); and horseradish peroxidase-labeled donkey anti-rabbit immunoglobulin G and donkey anti-mouse immunoglobulin G (Amersham Pharmacia Biotech, Piscataway, N.J.). Affinity-purified rabbit anti-claudin-5 was produced in the laboratory as described before (8).

MDCK II cells (obtained from Martin Schwartz) and PT67 cells (obtained from Clontech, Palo Alto, Calif.) were maintained in Dulbecco's modified Eagle's medium (DMEM) supplemented with 10% fetal bovine serum, 100 IU of penicillin per ml, and 100 μg of streptomycin per ml (Gibco-BRL, Rockville, Md.).

Site-directed mutagenesis of claudin-5 and construction of expression vector. Full-length mouse claudin-5 was cloned into the pLNCX vector (Clontech), and site-directed mutagenesis was performed with a Quikchange kit from Stratagene (La Jolla, Calif.) with the following oligonucleotide primer pairs (polyacrylamide gel electrophoresis purified, obtained from Sigma-Genosys, The Woodlands, Tex.). The primer pairs for substitution of Cys^{54} with Ser were 5′-GGGCTGT TGGATGTCGTCCGTGGTGCAGAGTACC-3′ and 5′-GGTACTCTGCACC ACGGACGACATCCACAGCCC-3′. The primer pairs for substitution of Cys^{64} with Ser were 5′-ACCGGGCACATGCAGTCCAAGGTGTATGAATCT-3′ and 5′-AGATTCATACACCTTGGACTGCATGTGCCCGGT-3′. The primer pairs for substitution of the Gln^{44} residue with Asn were 5′-CAACATCGTGA CGGCGAACACGACTTGGAAGGGGC-3′ and 5′-GCCCCTTCCAAGTCGT GTTCGCCGTCACGATGTTG-3′. The primer pairs for replacement of Leu^{50} and Trp^{51} with Gln and Arg, respectively, were 5′-ACGACTTGGAAGGGGC AAAGGATGTCGTGCGTGGT-3′ and 5′-ACCACGCACGACATCCTTTGC CCCTTCCAAGTCGT-3′.

For the double $Cys^{54}Cys^{64}$ mutant, the construct containing the Cys^{54} to Ser mutation was subsequently mutagenized to also change Cys^{64} to Ser. Molecular clones for each of the mutants were DNA sequence-verified. The pLNCX-based constructs were then transfected into PT67 cells (with Stratagene's MBS mammalian transfection kit) to produce retroviral particles containing the expression constructs. The virus-containing supernatant of transfected PT67 cell cultures was used for infection of MDCK II cells. Numerous G418-resistant clones were isolated for wild-type claudin-5 and each of the mutants as well as for cells containing the pLNCX retroviral vector alone, and three or four clones were analyzed for each, showing similar results. Immunostaining of all colonies selected for our experiments confirmed that the targeted protein was expressed in every single cell.

Protein electrophoresis and immunoblot. Confluent cells were dissolved in lysis buffer (60 mM Tris [pH 6.8], 150 mM NaCl, 2% sodium dodecyl sulfate, 1 mM dithiothreitol). After shearing with a 23-gauge needle, lysates were centrifuged at 5,000 × *g* at 4°C for 5 min, and the insoluble pellet was removed. Then, 15 μg of protein from each sample was subjected to sodium dodecyl sulfate-polyacrylamide gel electrophoresis under denaturing conditions and transferred to a nitrocellulose membrane or nylon membrane. After being blocked with 0.5% casein in Tris-buffered saline (TBS) for 1 h at room temperature, the protein blot was incubated with affinity-purified rabbit anti-claudin-5 (1:600), rabbit antiactin (1:50), or mouse antioccludin (1:5,000) in TBS (pH 7.4) at 4°C overnight, followed by incubation with horseradish peroxidase-labeled secondary antibody (1:10,000) at room temperature for 1 h. The positive bands were visualized with SuperSignal chemiluminescent substrate (Pierce, Rockford, Ill.) upon exposure to an X-OMAT LS film (Kodak Scientific Imaging System, New Haven, Conn.) or Hyperfilm (Amersham). Molecular weight determination was performed relative to ECL markers (Amersham).

Slot blot quantification. Serial dilutions of protein were diluted in TBS and applied to a nitrocellulose membrane (Osmonics Inc., Minnetonka, Minn.), with the aid of a Bio-dot SF cell apparatus (Bio-Rad, Hercules, Calif.) according to the manufacturer's recommendations. The membranes were blocked in TBS containing 3% gelatin at 30°C for 60 min, washed twice with TBS containing 0.05% Tween 20 (TBS-Tween), and dried, followed by rabbit anti-claudin-5 antiserum (1:800) or rabbit antiactin (1:400) in 1% gelatin in TBS-Tween. After washing with TBS-Tween, the membranes were incubated with horseradish peroxidase-labeled anti-rabbit immunoglobulin G (1:10,000) in 1% gelatin in TBS-Tween. The signal was visualized as above. Multiple exposures were performed to obtain intensities in the linear range. The relative quantification of band density was obtained on a digital image of the exposed film, analyzed by a Kodak 1D image analysis software (Eastman Kodak Co., New Haven, Conn.), similar to that described previously (58).

Deglycosylation. Cells samples were dissolved into lysis buffer (5 mM sodium phosphate [pH 7.5], 0.5% sodium dodecyl sulfate, 1% mercaptoethanol, and EDTA-free complete protease inhibitor cocktail) (Roche, Indianapolis, Ind.). After shearing with a 23-gauge needle, lysates were centrifuged at 5,000 × *g* at 4°C for 5 min, and the insoluble pellet was removed. The cell lysates were then denatured at 100°C for 10 min; 1/10 volume of 10% NP-40 was added to the cell lysate and mixed well. Peptide:*N*-glycosidase F (PNGase F; New England Biolabs Inc., Beverly, Mass.) (1 μl per 4 μg of cellular protein) was added to deglycosylate glycoproteins with N-linked carbohydrates and incubated at 37°C overnight, as per the manufacturer's specifications. PNGase F-treated and untreated samples were then analyzed by Western blot with detection with the rabbit anti-claudin-5 antibody or the rabbit antiactin antibody, as above.

Immunolabeling and confocal microscopy. Cells grown on glass chamber slides were fixed with 10% formalin in phosphate-buffered saline (PBS) for 10 min at room temperature, followed by incubation with 0.2% Triton X-100 in TBS for 10 min (46). The cells on these slides were blocked with PBS containing 0.5% casein, 10% normal fetal bovine serum, and 1% bovine serum albumin at room temperature for 1 h. The cells were then incubated with individual antibodies or combinations of primary antibodies: goat anti-ZO-1 antibody (1:200) plus either rabbit anti-claudin-1 antibody (1:200), mouse anti-claudin-2 antibody (1:300), mouse anti-claudin-4 antibody (1:300), mouse anti-claudin-5 antibody (1:200), or rabbit antioccludin antibody (1:200); in the blocking solution at 4°C overnight or at room temperature for 1 h. Labeling with anti-mouse IgG-Texas Red (1:700) or anti-rabbit IgG-Texas Red (1:700) and/or anti-goat IgG-fluorescein isothiocyanate (1:500) in PBS followed at room temperature for 1 h. After washing with PBS, slides were mounted with ImmunoFluor (ICN, Costa Mesa, Calif.) and viewed under fluorescence confocal microscopy (MRC1024; Bio-Rad).

Measurement of TER, paracellular ion conductivity, and dilution potentials. TER was determined with Endohm electrodes (World Precision Instruments, Sarasota, Fla.). The resistance of the confluent monolayer of cells in a Millicell insert (Millipore, Bedford, Mass.) was measured in buffer (20 mM HEPES buffer, pH 7.0, containing 3 mM $CaCl_2$, 10 mM glucose, and 1 mM sodium pyruvate) containing 165 mM chloride salt of lithium, potassium, rubidium, sodium, or cesium. Ion conductance is represented as the reciprocal of resistance between buffers containing the various ions in two compartments (conductance $G = 1{,}000 \times 1/\mathrm{TER}$). All solutions were made at an osmolality of 333 mos mol/kg H_2O, verified with an Advanced Laboratory wide-range osmometer (Advanced Instrument, Needham Heights, Mass.). TER was measured in 20 mM HEPES-buffered DMEM (pH 7.0), before and after each buffer to verify that the monolayers were unaltered during the experiment. Filters were washed three times for each buffer change. Dilution potentials were measured by substitution of mannitol for 50% of the NaCl in one chamber while preserving osmolality. Electrical potentials were measured with buffer A (120 mM NaCl, 10 mM

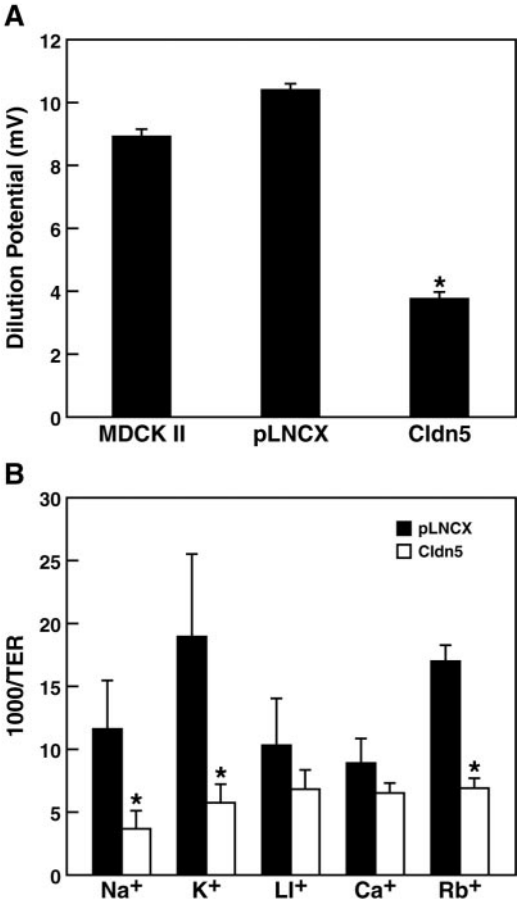

FIG. 1. Paracellular conductance of ions. (A) The 50% dilution potentials were measured in parental MDCK II cells, control MDCK II cells containing the pLNCX vector, and MDCK II cells expressing claudin-5. Expression of claudin-5 significantly decreased dilution potentials compared to parental cells and to cells with the pLNCX vector (one-way analysis of variance combined with Bonferroni *t* tests; $n = 6$, $P < 0.001$). (B) Paracellular conductance of group Ia alkali cations. Claudin-5 expression dramatically reduced the ionic conductance of sodium and potassium in the paracellular pathway. There was a statistically significant difference in conductance of sodium ions, potassium ions, and rubidium ions between pLNCX transductants and claudin-5 transductants. Data are presented as mean ± standard deviation (one-way analysis of variance combined with Bonferroni *t* tests; $n = 4$, $P < 0.001$).

HEPES [pH 7.4], 5 mM KCl, 10 mM $NaHCO_3$, 1.2 mM $CaCl_2$, 1 mM $MgSO_4$) on the basal side of the culture chamber and buffer B (60 mM NaCl, 120 mM mannitol, 10 mM HEPES [pH 7.4], 5 mM KCl, 10 mM $NaHCO_3$, 1.2 mM $CaCl_2$, 1 mM $MgSO_4$) on the apical side of the chamber. Electrical potentials obtained from blank inserts were subtracted from those obtained from inserts with confluent growth of cells.

Paracellular flux measurement. Paracellular flux for mannitol was measured as described before (5). Briefly, after growing to confluence (confirmed with TER measurement), cells cultured in a Millicell insert within a 24-well plate were washed with 300 μl of P buffer (10 mM HEPES [pH 7.4], 1 mM sodium pyruvate, 10 mM glucose, 3 mM $CaCl_2$, 145 mM NaCl), and the outer well was washed with 500 μl of P buffer. The Millicell was then placed in a new 24-well plate containing 500 μl of P buffer per well; 250 μl of P buffer containing 2 mM cold mannitol and 10 μCi of [^{3}H]mannitol per ml was applied to the apical compartment of the cell in the Millicell insert. Under these conditions, linearity of measurements, taken every 30 min, was achieved over at least 120 min, and for experimental determination, cells were incubated at 37°C and 5% CO_2 for 2 h. We subsequently added 100 μl of P buffer removed from the basal compartment of the Millicell to 3 ml of ScintiVerse (Fisher Scientific, Pittsburgh, Pa.) to determine the radioactivity level. Finally, samples were counted on a Beckman LS6500 multipurpose scintillation counter (Beckman, Fullerton, Calif.).

Paracellular flux for monosaccharides of different charges was performed as described by others (6). Four radiolabeled molecules were used in the assay: 3-*O*-[methyl-^{3}H]-D-glucose and D-[6-^{3}H(*N*)] glucosamine hydrochloride (NEN Life Science Products, Boston, Mass.), and *N*-[9-^{3}H] sialic acid and D-[1-^{14}C] mannitol (American Radiolabeled Chemicals, St. Louis, Mo.). The assay was performed by adding 3 μCi of [^{14}C]mannitol per ml alone or 3 μCi of [^{14}C]mannitol per ml mixed with 3 μCi of [^{3}H] monosaccharide per ml to 250 μl of P buffer (containing 2 mM unlabeled mannitol and 2 mM unlabeled monosaccharide corresponding to the ^{3}H-labeled preparation) and applied to the apical chamber of the Millicell containing confluent cells; 500 μl of P buffer was added to the basal chamber of the Millicell. The P buffer used in the latter assay contained 0.25 mM phloretin. Alternatively, 50 μM chloroquine was added to P buffer for the assay with *N*-[9-^{3}H]sialic acid as a tracer. Phloretin and 25 mM glucose were added to the incubation buffer to inhibit the transcellular transport of methylglucose and glucosamine (46); chloroquine was used to prevent the vesicular traffic of sialic acid (3). These substances had no effect on the paracellular pathway, as found in previous studies (6, 55).

After incubation at 37°C in 5% CO_2 for 1.5 h, 100 μl of P buffer was removed from the basal compartment of the Millicell and added to 3 ml of ScintiVerse. Radioactivity levels of ^{3}H and ^{14}C were measured simultaneously and then counted separately with a Beckman LS8501 multipurpose scintillation counter.

Manipulation of extracellular redox potential. Cells were grown to confluency as above and then switched to methionine-, cysteine-, and cystine-free DMEM supplemented with 30 mg of methionine per liter, 10% fetal bovine serum, 100 IU of penicillin per ml, and 100 μg of streptomycin per ml. Media with a range of extracellular redox states (E_h) were obtained by varying the extracellular thiol/disulfide pool while maintaining a total concentration of cysteine moieties (cysteine plus [2 × cystine]) at 200 μM (30). With the Nerst equation, the following concentrations (micromolar) of cystine/cysteine were used to achieve a given E_h: 99.75/0.5 for 0 mV, 98/4 for −46 mV, 80/40 for −109 mV, and 10/180 for −150 mV (30). Following the addition of cystine/cysteine, the medium was adjusted to pH 7.4, filter sterilized, and used immediately. TER was measured before and after 24 h of defined redox medium addition; the medium was then changed to the same redox concentrations for measurement of mannitol flux.

RESULTS

Claudin-5 increases TER by decreasing conductance of alkali metal cations. MDCK II cells expressing wild-type claudin-5 exhibited a significant fivefold increase in TER compared to the parental cells (relative TER ratios of three independent clones of claudin-5 transductants, 5.0 ± 1.6; vector-only

```
(aa#): 30        40        50        60        70        80
        *         *         *         *         *         *
Cldn5  PMWQVTAFLDHNIVTAQTTWKGLWMSCVVQSTGHMQCKVYESVLALSAEVQAAR
Mut1   PMWQVTAFLDHNIVTAQTTWKGLWMS***S***VVQSTGHMQCKVYESVLALSAEVQAAR
Mut2   PMWQVTAFLDHNIVTAQTTWKGLWMSCVVQSTGHMQ***S***KVYESVLALSAEVQAAR
Mut3   PMWQVTAFLDHNIVTAQTTWKGLWMS***S***VVQSTGHMQ***S***KVYESVLALSAEVQAAR
Mut4   PMWQVTAFLDHNI***M***TAQTTWKGLWMSCVVQSTGHMQCKVYESVLALSAEVQAAR
Mut5   PMWQVTAFLDHNIVTA***N***TTWKGLWMSCVVQSTGHMQCKVYESVLALSAEVQAAR
Mut6   PMWQVTAFLDHNIVTAQTTWKG***QR***MSCVVQSTGHMQCKVYESVLALSAEVQAAR
```

FIG. 2. Predicted amino acid sequence of the first ECD in wild-type claudin-5 and its mutants. Residues altered by site-directed mutagenesis are indicated in bold italics.

pLNCX transductants, 1.3 ± 0.5; and parental MDCK II cells, 1.0 ± 0.1). This indicates that claudin-5 dramatically enhanced the barrier's obstruction of electrical conductance, decreasing ionic permeability across TJs between adjacent MDCK II cells. To determine the ionic conductance changes resulting from claudin-5 expression, measurements of 50% dilution potentials were performed in claudin-5 transductants, creating an NaCl concentration gradient without an osmotic gradient. As shown in Fig. 1A, the dilution potential obtained in claudin-5 transductants was significantly less than those found in control pLNCX transductants or parental MDCK II cells (42 and 36%, respectively), indicating that claudin-5 selectively decreased the relative permeability of Na^+ cations compared with Cl^- anions.

Measurements of cationic conductivity were then performed with cesium chloride, rubidium chloride, lithium chloride, potassium chloride and sodium chloride. As shown in Fig. 1B, the conductance of the lighter alkali metal cation elements was significantly reduced in claudin-5-expressing cells. Potassium and sodium conductance was reduced to 32 and 30%, respectively, in claudin-5 transductants compared to control pLNCX transductants, whereas rubidium conductance was reduced to 41% of that in controls. However, conductance of cesium and lithium did not significantly decrease in claudin-5 transductants (73 and 66% of pLNCX transductants, respectively).

Expression of mutant claudin-5 in MDCK II cells. The first predicted ECD of the claudins contains several conserved amino acid residues. To elucidate the contribution of certain amino acids to the functions of claudin-5 protein as well as the properties of the first ECD, mutations were introduced into the mouse claudin-5 cDNA by site-directed mutagenesis. Thereafter, expression constructs containing these claudin-5 mutants were transduced into MDCK II cells. Three independent clonal lines were established for each construct, and all three lines created for each construct had demonstrably similar properties.

Five claudin-5 mutants generated by site-directed mutagenesis of the first ECD and a sixth mutant obtained from a random PCR-induced change in the first ECD were studied (Fig. 2). Three of these mutants were designed to examine the roles of the cysteines: mutation (Mut)1 (Cys^{54}→Ser^{54}) replaced the first cysteine residue of claudin-5 ECD with serine; in Mut2 (Cys^{64}→Ser^{64}), the second cysteine residue was replaced; and Mut3 (Cys^{54}→Ser^{54}, Cys^{64}→Ser^{64}) replaced both cysteines. Three additional mutations were also investigated: Mut4, with a randomly created mutation in claudin-5 (Val^{41}→Met^{41}); Mut5, which introduced a potential N-linked glycosylation site in claudin-5 by substituting Asn for the Gln^{44} residue, creating an Asn^{44}-X-Thr^{46} motif; and Mut6, with increased hydrophilic character and charge after replacement of Leu^{50} and Trp^{51} with Gln^{50} and Arg^{51}.

Figure 3 shows immunostaining of claudin-5 and the mutants in transductants. No positive staining for claudin-5 was seen in the parental MDCK II cells or in cells transduced with the pLNCX vector alone (Fig. 3A1). Introduction of wild-type claudin-5 (Fig. 3B1), led to expression that was targeted to the lateral plasma membrane region, being predominantly colocalized with ZO-1 (Fig. 3B) in the TJ complex. With the exception of Mut5, the claudin-5 mutants showed similarly predominant colocalization with ZO-1. Mut5, which contains a consensus

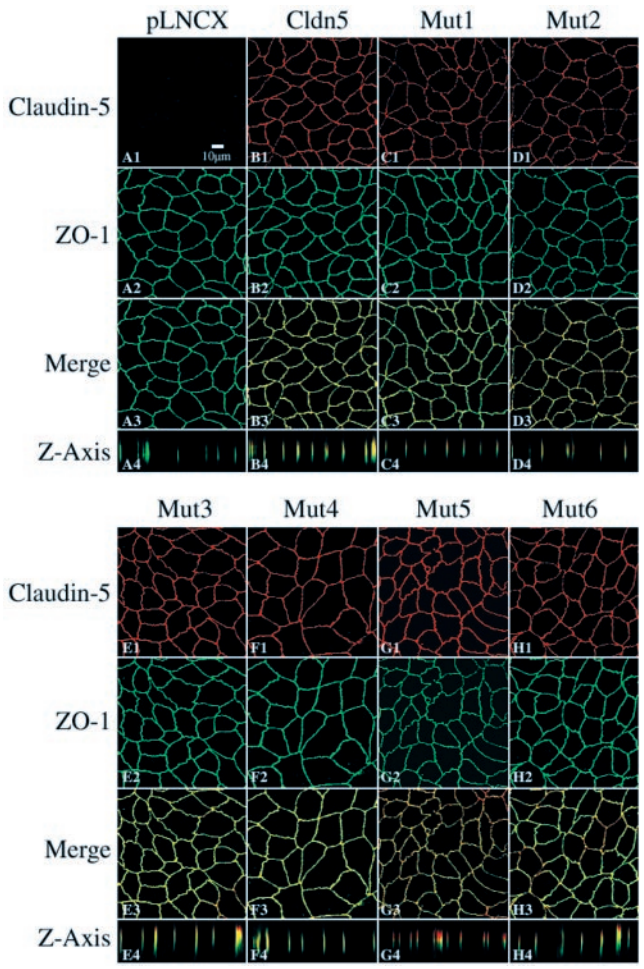

FIG. 3. Confocal microscopic images of claudin-5 wild-type and mutants expressed in MDCK II cells following immunofluorescent labeling for ZO-1 and claudin-5. The TJs were localized by ZO-1 expression visualized with fluorescein isothiocyanate. Claudin-5 expression was visualized with Texas Red. Transductants with a blank pLNCX vector were negative for claudin-5 labeling (A). In wild-type claudin-5 transductants, claudin-5 stained with Texas Red colocalized with ZO-1 (B). The patterns of immunolocalization in the claudin-5 mutants Mut1 to Mut6 are presented in panels C to H. Rows 1 to 3 represent images in the *x-y* plane taken at the midpoint of ZO-1 localization; row 4 represents computer reconstruction of the *x-z* plane. Bar, 10 μm.

N-linked glycosylation site in the first ECD, is largely localized apical to ZO-1, although overlap with ZO-1 immunostaining is still present (Fig. 3G4).

Occludin and other claudins are also endogenously expressed in MDCK II cells. Figure 4 shows immunostaining of the other claudins known to be expressed in MDCK II cells (claudins-1, -2, and -4) as well as occludin in the control, wild-type claudin-5, and individual cysteine mutant (Mut1 and Mut2)-expressing MDCK II cells. When the pLNCX vector, exogenous wild-type, or mutant claudin-5 was introduced into MDCK II cells, endogenous claudin-1 was still observed along the plasma membrane and remained colocalized with the TJ protein ZO-1 (Fig. 4A to D). No significant difference was found in the intensity and distribution patterns of claudin-1 between controls (pLNCX transductants) and wild-type, Mut1,

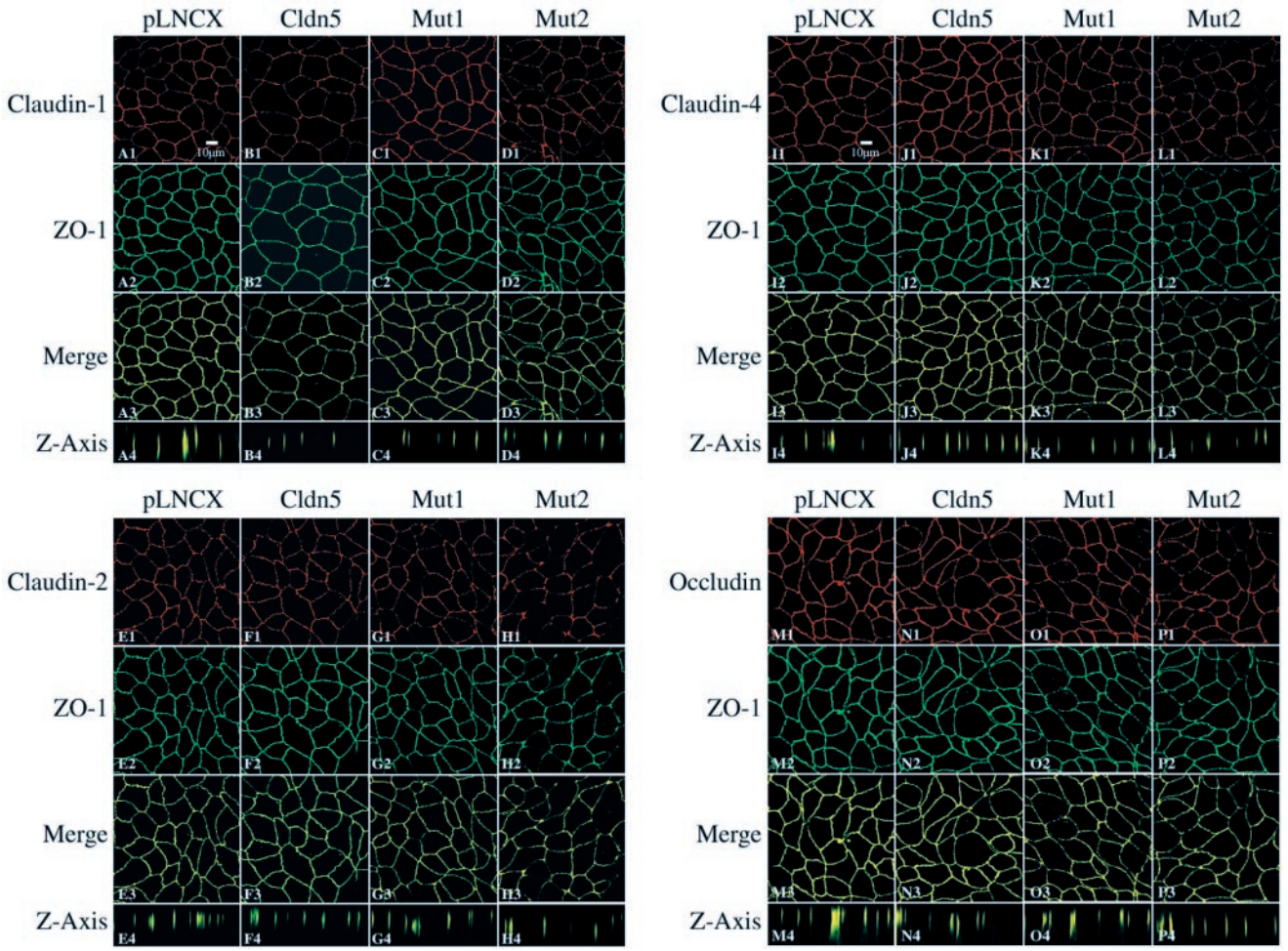

FIG. 4. Confocal microscopic images of claudin-5 wild-type and mutants expressed in MDCK II cells following immunofluorescent labeling for ZO-1 and other claudins and occludin. The TJs were localized by ZO-1 expression visualized with fluorescein isothiocyanate. Claudin-1 (panels A to D), claudin-2 (panels E to H), claudin-4 (panels I to L), and occludin (panels M to P) were visualized with Texas Red. Images were performed as per the Fig. 3 legend.

or Mut2 claudin-5 transductants. Similarly, we did not observe any significant alterations in the expression of claudin-2, claudin-4, or occludin after expression of either wild-type claudin-5, Mut1, or Mut2 (Fig. 4E to P).

Immunoblot analysis revealed that exogenous claudin-5, whether wild type or produced by Mut1 to Mut4, was expressed in the transduced MDCK II cells as an approximately 23-kDa protein (Fig. 5A). Mut6 also migrated identically (not shown). Analysis of Mut5, which contains the consensus N-linked glycosylation site, exhibited, in addition to the 23-kDa protein, a slower-migrating species (centered on approximately 35 kDa) (Fig. 5A). This additional larger band of Mut5 was eliminated by treatment with PNGase F (Fig. 5B), an amidase that cleaves between the innermost GlcNAc and the asparagine residue in N-linked glycoproteins, indicating that the additional band was indeed caused by N-linked glycosylation of claudin-5. Glycosylation of this introduced site supports the predicted extracellular localization of this region of the claudin protein.

Although expression of the exogenous wild-type or mutant claudin-5 proteins could be found colocalized with ZO-1, the total amount of claudin-5 in the cells varied between the different cloned cell lines. When quantified relative to actin (e.g., Fig. 5C), the expression level in different clones for wild-type claudin-5 and Mut1 to Mut5 overlapped, exhibiting a sixfold range of expression. However, claudin-5 levels in cellular clones expressing Mut6 were always at levels lower than those found for the other constructs.

Conserved cysteines in the first ECD are critical in claudins-5's function. We then examined selected amino acid residues in the first ECD for their contribution to the tightening of the barrier by claudin-5 (Fig. 6). When expressed in MDCK II cells, neither Mut1, Mut2, nor Mut3, which lacked Cys^{54} and/or Cys^{64}, increased TER, indicating that these conserved cysteine residues were essential for the enhanced barrier function resulting from the expression of claudin-5 in TJs. Expression of Mut4 yielded a significant fourfold increase in TER (comparable to the fivefold increase with wild-type claudin-5), indicating that this relatively conserved random mutation did not change the ability of claudin-5 to decrease ionic permeability between adjacent cells. Neither Mut5, resulting in glycosylation of the first ECD, nor Mut6, replacing the conserved

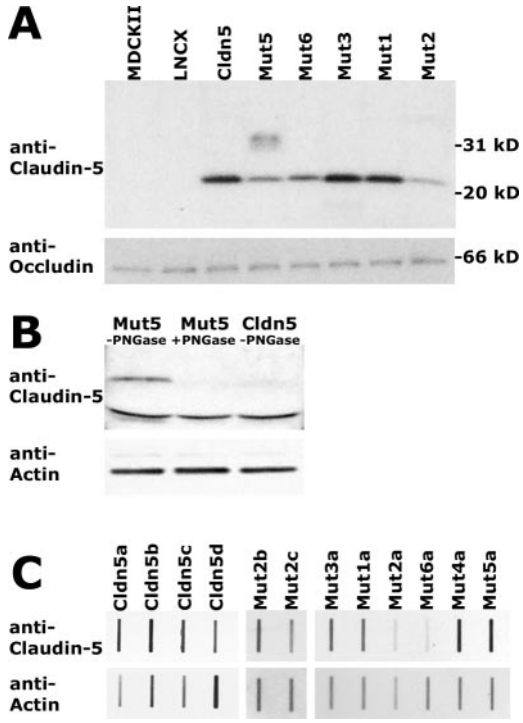

FIG. 5. Immunoblot analysis of exogenous claudin-5 protein expression in MDCK II cells. Western blot analysis of wild-type claudin-5, Mut1 to Mut3, and Mut6 revealed a distinct band of 23-kDa, seen after reaction with anti-claudin-5, visualization with ECL, and exposure to X-ray film (A, upper). Mut5, containing a consensus glycosylation site, exhibited an additional diffuse band centered around 35 kDa (A, upper). The blot was stripped and incubated with antioccludin with visualization as above, resulting in a band of 66 kDa (A, lower). Similar Western blot analysis indicating that the slower-migrating species in Mut5-expressing cells is eliminated following digestion with PNGase F (B, upper). The blot was stripped and incubated with antiactin (B, lower). Quantification of claudin-5 expression in individual cell clones was performed by slot blot analysis, with serial dilutions of total cell extracts incubated with anti-claudin-5 or antiactin and visualized by ECL with multiple exposures to film to obtain data in the linear range of densitometry. Examples of the data are shown (C), with the different lowercase letters indicating independent cellular clones expressing a given construct.

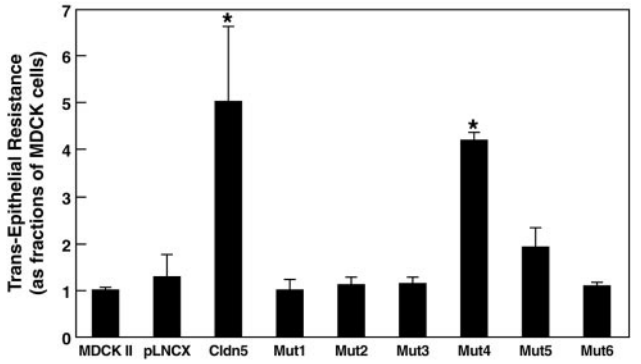

FIG. 6. TER of wild-type and mutant claudin-5 transductants. Wild-type claudin-5 transductants exhibited a significant fivefold increase in TER, and Mut4 (with random mutation) transductants had a fourfold increase; the other claudin-5 mutants had no significant alterations. Data are shown as means ± standard deviation (one-way analysis of variance combined with Bonferroni t tests; $n = 3$, $P < 0.001$).

LW residues to ones with increased hydrophilicity, could change the TER when expressed in MDCK II cells.

Although differences in the expression levels of claudin-5 and its mutants might affect TJ function in the transductants, examination of independent clones for a given construct revealed no link between relative expression level (within the range examined) and effects on TJ function. For example, four independent wild-type claudin-5 transductants varied threefold in relative expression level, but the TERs varied less than twofold. The two clones with the highest and lowest TERs had similar expression levels of claudin-5, whereas the two clones with the most divergent expression differed by only 20% in TER. However, as noted previously, the expression levels of Mut6 did not reach those of the other constructs.

Cysteine residues can exist in numerous oxidation and ionization states in proteins due to cysteine's redox activity and nucleophilicity. The local redox state can significantly affect the function of cysteine-containing proteins (21). To test whether the barrier function in MDCK II cells is sensitive to changes in the extracellular redox conditions, we manipulated the extracellular thiol and disulfide concentrations of the medium to achieve redox states (E_h) ranging from 0 to −150 mV. However, neither control transductants (pLNCX, data not shown) nor claudin-5-containing cells (TER at 0 mV = 576 ± 43.6 Ωcm^2; TER at −46 mV = 536 ± 22.1 Ωcm^2; TER at −109 mV = 577 ± 27.0 Ωcm^2; TER at −150 mV = 557 ± 13.7 Ωcm^2) exhibited redox-sensitive changes in TER.

Paracellular flux is dramatically increased after substitution of serine for Cys[64]. Restriction of paracellular molecular flux is one of the most important characteristics of TJs. To trace paracellular flux here, we used mannitol because it is nonionic and has no known transporter in transcellular membrane pathways (36). With [^{3}H]mannitol, paracellular flux was measured across the cell layer of MDCK II cells expressing wild-type claudin-5 or its mutants.

Expression of wild-type claudin-5, Mut1 (first cysteine), Mut3 (both cysteines), Mut4 (random), Mut5 (glycosylation), and Mut6 (hydrophilic) did not significantly alter mannitol flux compared to that of cells expressing the vector alone (Fig. 7). In contrast, expression of Mut2 (second cysteine) resulted in a greater than threefold increase in mannitol flux (370% of the control value; Fig. 7), indicating significantly decreased TJ restriction to paracellular nonionic molecular flux. Like that on the TER, the effect of Mut2 on mannitol flux was not dependent on the Mut2 expression level. Furthermore, restriction of mannitol flux in control and claudin-5-expressing cells was not redox sensitive (data not shown).

In order to determine whether the paracellular flux change induced by Mut2 was influenced by ionic charge, the ability of ^{3}H-labeled monosaccharides with different charge states to permeate the cells at cell culture pH, methylglucose (neutral molecule), glucosamine (60% positively charged), and sialic acid (100% negatively charged), was measured relative to that of the mannitol to control for the increased permeability of Mut2. Although the rank order of paracellular flux of monosaccharides in pLNCX, wild-type claudin-5, or Mut 2 transductants was the same (glucosamine > glucose > sialic

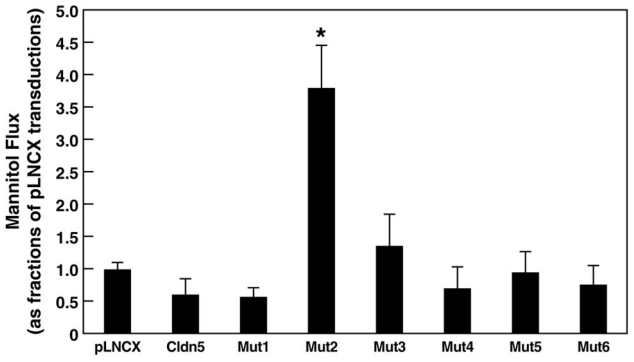

FIG. 7. Paracellular flux of mannitol in MDCK II cells expressing claudin-5 or its mutants. Only Mut2 (Cys^{64}) transductants exhibited a significant difference from controls, a 3.7-fold increase in mannitol flux. Data are shown as means ± standard deviation (one-way analysis of variance combined with Bonferroni *t* tests; $n = 3$, $P < 0.001$).

acid, data not shown), the relative permeability to the negatively charged sialic acid was significantly increased, and the relative permeability to the positively charged glucosamine decreased significantly, by Mut2 relative to either pLNCX or wild-type claudin-5 (Fig. 8). Thus, TJs with claudin-5 Mut2 lost barrier function for monosaccharides, with preferential enhancement for negatively charged molecules.

DISCUSSION

TJs containing claudin-5 exhibit altered barrier function and molecular conductivity. In our present study, the TJ integral membrane protein claudin-5, which is found predominantly in endothelial cells, was expressed in the MDCK epithelial cell line. Similar to BBB endothelial cells, MDCK cells express occludin, ZO-1, and other components of TJ formation

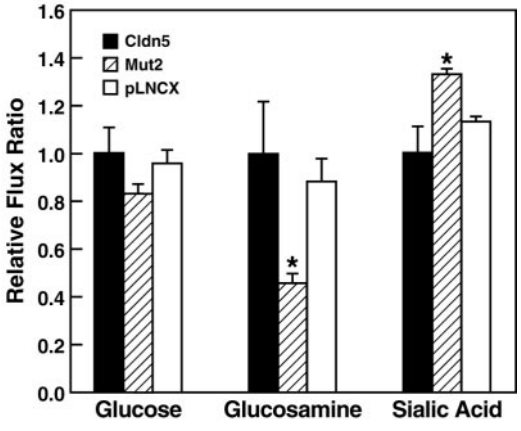

FIG. 8. Relative paracellular flux of uncharged and charged monosaccharides in MDCK II cells expressing the pLNCX vector, wild-type claudin-5, or Mut2. Mut2-expressing cells showed increased paracellular flux of all monosaccharides. Normalized to the flux of mannitol, the Mut2 transductants were significantly more permeable to the negatively charged sialic acid ($F = 15.84$, $P = 0.004$) and less permeable to the positively charged glucosamine ($F = 12.06$, $P = 0.008$) than were the vector pLNCX or wild-type claudin-5 transductants (one-way analysis of variance combined with post hoc Bonferroni *t* test; $n = 3$; $P < 0.05$ for between-two-group comparisons).

and function; strong physiological analogies have been drawn between the capillary endothelium comprising the BBB and the kidney tubule epithelium (15), from which MDCK cells derive. Expression of claudin-5 was associated with a dramatic fivefold increase in TER over that of the parental cells. Such increased resistance mediated by the TJs was dependent upon critical residues, notably the cysteines, in the first ECD of claudin-5.

It is believed that the TER obtained from relatively low resistance epithelia largely reflects the permeability of the paracellular pathway gated by TJs (22, 47). Accordingly, under the conditions of MDCK II cell culture, the main change in resistance across a single cell layer was considered a result of changes in the paracellular rather than in the transcellular pathway. Therefore, the increased TER in claudin-5 transductants found here stemmed from alterations of the electrical conductive properties of TJs that gate the paracellular flux. Our finding that the alterations in TJ flux resulted from incorporation of exogenous claudin-5 into TJs in MDCK II cells was strongly supported when specific mutations introduced into the first ECD of claudin-5 in MDCK II cells abolished the elevated TER observed in transductants expressing wild-type claudin-5.

Others have demonstrated that TER is determined either by the amounts of claudins or occludin and numbers of TJ complexes or strings on adjacent cells or by the varied arrangements and types of claudin members in TJs (20). Furthermore, it has recently been demonstrated that the TJ fibril number does not correlate to changes in TER; rather, it is dependent upon the ECDs of the claudins (11). Our findings with claudin-5 expression and the first-ECD mutants expand upon these studies. Expressing exogenous claudin-5 did not alter the expression patterns of endogenous occludin or claudins in MDCK II cells. Claudin-1, claudin-2, claudin-4, and occludin were all observed at very similar immunostaining levels in all transductant cells expressing claudin-5 or its mutants compared with transductant cells expressing blank pLNCX vector alone. This is in contrast to the recently reported expression of claudin-8 in MDCK II cells, which significantly downregulates claudin-2 expression (59). The alterations observed in MDCK II cells likely resulted directly from the expression of claudin-5 rather than by altering the endogenous TJ proteins from the TJs in MDCK II cells, at least for the proteins amenable to the current analysis.

Our results contrast with a recent study in which claudin-5 was introduced in NIH 3T3 fibroblasts and IB3.1 cells, an airway epithelial line. Expression of claudin-5 in these cell lines did not change TER but increased the paracellular permeability (13). However, neither of these cell lines forms TJs. Our findings, in the context of functional TJs in MDCK II cells, reflect the physiological effect of claudin-5 in the presence of a TJ barrier. It is likely that, in the absence of TJs, claudin-5 expression can lead to other properties.

Although we found a fivefold increase in TER, no significant decreases in paracellular flux were observed in the claudin-5 transductants. Furthermore, the 3.7-fold increase in paracellular flux obtained with claudin-5 Mut2 was not accompanied by an alteration in TER. These findings verified one important characteristic of TJs observed in previous studies, dissociation between changes in the barrier properties of conductance for ionic molecules and flux for neutral molecules. For example, a

paradoxical increase in mannitol flux was obtained in transductants expressing Myc-tagged claudin-1 that exhibited a decreased ionic permeability (an increase in TER) (38). Also, expression of claudin-4 and occludin increased TER without altering mannitol flux, whereas partially depleted occludin in a transductant decreased mannitol flux in parallel with a reduced TER (4, 54).

These divergent phenomena may be due to a number of factors. Aqueous pores in TJ strands may fluctuate between open and closed states (10). Mannitol and other tracer molecules can transit pores in TJ strands one by one over time, and the prolonged (over hours) assessment of paracellular flux measures the accumulation of molecules undergoing passive passage. In contrast, the instantaneous TER requires that aqueous pores in TJ strands remain open during this transient time of measurement. Thus, TER is a measure of the open or closed state of paracellular pathways in a cell monolayer during the instant of testing. Still, the TER is the average of a large number of such pathways, and the technical differences in the instantaneous versus prolonged measurements may not explain such results. Furthermore, it is not clear that the same molecular pathway is utilized by ions as opposed to larger molecules. Interestingly, when claudins are exogenously expressed in fibroblasts, the dynamic behavior of the polymerized paired strands can be observed (49). Biochemical analysis of claudin-4 produced in insect cells revealed a labile nature of the claudin oligomer, implying a dynamic state (39). Although performed in experimental settings removed from functional TJs, both studies suggest a means by which the dynamic behavior of claudin-based TJs can allow the flux of molecules while retaining the structure of TJs and dissociate flux from TER.

TJs of the BBB. Our original identification of MBEC1/claudin-5 mRNA and protein expression by the endothelial cells of the BBB (8) has subsequently been confirmed by others (34, 41, 42). In addition to BBB and other endothelial cells, our studies (8) and those of others (32, 35, 45, 56) have revealed claudin-5 expression in epithelial cells as well as other specialized cell types, including pancreatic acinar cells (45) and myelinating Schwann cells in nerves (44).

A functional role of claudin-5 in the BBB has just been reported (43). In this study, claudin-5 expression was genetically knocked out in mice, and such animals developed normally but died shortly after birth. Interestingly, although brain endothelial TJs appeared to form normally, studies on day 18.5 embryos revealed that the BBB was now abnormally leaky to molecules with a mass of less than 800 Da. Due to the lethality, potential BBB abnormalities could not be examined in the mature BBB, for example, when occludin expression is upregulated. Interestingly, occludin knockout mice are able to form TJs, although BBB abnormalities have not been examined in these mice (48). More studies are necessary to clearly delineate the roles of occludin, claudin-5, and other TJ proteins in BBB function.

The presence of claudin-5 in endothelial cells in association with other TJ protein components, such as occludin and ZO-1, as found in both the MDCK cell line and BBB endothelial cells, may form the highly restrictive barrier that prevents an exchange of molecules via the paracellular pathway between the circulatory system and the central nervous system and represent one of the molecular mechanisms of the BBB. Several lines of evidence support the critical roles of claudin-5 in functions of TJs in brain endothelial cells: the recognition that claudins are critical components of TJs, and the identification of claudin-5, occludin, and ZO-1 at the TJ in BBB endothelia, the functional change in embryonic BBB endothelial TJ resulting from claudin-5 deletion, and the ability of claudin-5, when expressed in conjunction with occludin, ZO-1, and other TJ proteins, to increase TJ-mediated TER, as reported here.

Molecular analysis of claudin-5. We analyzed the molecular basis for claudin-5 function by introducing mutations within claudin-5 with site-directed mutagenesis. We concentrated on characterizing the first ECD of claudin-5, specifically the two cysteine residues, Cys^{54} and Cys^{64}, that are conserved in every claudin family member. Since cysteines residues are critical in the folding patterns and functions of many channel proteins (7, 9, 25, 33), these two residues and their neighboring residues were examined here for their possible involvement in claudin-5's structure and functional domains. It has already been shown that these cysteines are necessary for claudin-5 to activate matrix metalloproteinase 2 (40), since deletion of the domain containing these two cysteines in claudin-1 abolished such activation. This outcome led to the proposal that cysteines might be crucial for the functions of claudin-5 in vascular permeability, for instance, in the BBB, through interactions between claudins and matrix metalloproteinase 2.

It was striking that a mutation changing Cys^{64} changed the properties of electrical barriers and monosaccharide barriers, producing lower TER and higher monosaccharide flux in the paracellular pathway compared with those in the claudin-5 wild-type transductants. Unlike the mutations in the other sites of claudin-5, which caused only a loss of ability to increase resistance to ionic flux, a mutation in Cys^{64} eliminated the ability of claudin-5 to increase the electrical barrier and simultaneously decreased the obstruction in monosaccharide flux at the TJ. These claudin-5 Mut2 transductants increased the paracellular flux of charged as well as uncharged monosaccharides, showing a preference for negatively charged molecules, although the TER in claudin-5 Mut2 transductants did not change compared with that of the control.

These data on TER and monosaccharide flux strongly imply that claudin-5 might discriminate among charged molecules and restrict passage to those selected. Interestingly, the charged residues in the first ECD of claudins have been shown to determine paracellular charge selectivity at the TJ (12). Here we have examined the uncharged residues within the first ECD. Whereas Cys^{54} is necessary for claudin-5 to increase TER, we found that Cys^{64} in claudin-5 is required both for functionally isolated barriers to electrical conductance and for monosaccharide passage. Thus, several barrier functions in TJs might have a common molecular basis in the first ECD of claudin-5. However, as the ultrastructural basis of pores in TJs is unknown, ions and solutes may traverse similar or distinct structures to traverse the paracellular space (23), the molecular nature of the different functions of TJs remains speculative.

In contrast to the critical Cys^{64} mutation, mutations of the other amino acid residues demonstrated only their probable involvement in the generation of electrical restriction in TJs. Moreover, given that the mutation of Cys^{54} in claudin-5 did not show the same effect as the mutation of Cys^{64}, the possibility that simple disruption of the intramolecular disulfide bond

between Cys^{54} and Cys^{64} is responsible for increased molecular flux was eliminated. Furthermore, we could not demonstrate redox-mediated alterations in TJ function under the conditions examined. Thus, the cysteines may affect function through the formation of intermolecular disulfide bonds with cysteine from claudin-5, other claudins, or other protein molecules, binding of metal ions such as zinc, or through chemical modification such as nitrosylation. Finally, since disruption of Cys^{64} interactions led to selective opening of the paracellular pathway, perhaps TJs can be opened for therapeutic purposes, such as allowing drugs to penetrate the BBB.

ACKNOWLEDGMENTS

This work was supported by NIH grants NS37567 and MH62261.

REFERENCES

1. **Anderson, J. M.** 2001. Molecular structure of tight junctions and their role in epithelial transport. News Physiol. Sci. **16:**126–130.
2. **Anderson, J. M., and C. M. Van Itallie.** 1995. Tight junctions and the molecular basis for regulation of paracellular permeability. Am. J. Physiol. **269:**G467–G475.
3. **Antohe, F., L. Dobrila, C. Heltianu, N. Simionescu, and M. Simionescu.** 1993. Albumin-binding proteins function in the receptor-mediated binding and transcytosis of albumin across cultured endothelial cells. Eur. J. Cell Biol. **60:**268–275.
4. **Balda, M. S., C. Flores-Maldonado, M. Cereijido, and K. Matter.** 2000. Multiple domains of occludin are involved in the regulation of paracellular permeability. J. Cell Biochem. **78:**85–96.
5. **Balda, M. S., J. A. Whitney, C. Flores, S. Gonzalez, M. Cereijido, and K. Matter.** 1996. Functional dissociation of paracellular permeability and transepithelial electrical resistance and disruption of the apical-basolateral intramembrane diffusion barrier by expression of a mutant tight junction membrane protein. J. Cell Biol. **134:**1031–1049.
6. **Ban, Y., and L. J. Rizzolo.** 2000. Differential regulation of tight junction permeability during development of the retinal pigment epithelium. Am. J. Physiol. Cell. Physiol. **279:**C744–C750.
7. **Benitah, J. P., G. F. Tomaselli, and E. Marban.** 1996. Adjacent pore-lining residues within sodium channels identified by paired cysteine mutagenesis. Proc. Natl. Acad. Sci. USA **93:**7392–7396.
8. **Chen, Z., M. Zandonatti, D. Jakubowski, and H. S. Fox.** 1998. Brain capillary endothelial cells express MBEC1, a protein that is related to the Clostridium perfringens enterotoxin receptors. Lab. Investig. **78:**353–363.
9. **Choi, Y., H. V. Chen, and S. A. Lipton.** 2001. Three pairs of cysteine residues mediate both redox and Zn^{2+} modulation of the nmda receptor. J. Neurosci. **21:**392–400.
10. **Claude, P.** 1978. Morphological factors influencing transepithelial permeability: a model for the resistance of the zonula occludens. J. Membr. Biol. **39:**219–232.
11. **Colegio, O., C. Van Itallie, C. Rahner, and J. Anderson.** 2003. Claudin extracellular domains determine paracellular charge selectivity and resistance but not tight junction fibril architecture. Am. J. Physiol. Cell. Physiol. **284:**C1346–C1354.
12. **Colegio, O. R., C. M. Van Itallie, H. J. McCrea, C. Rahner, and J. M. Anderson.** 2002. Claudins create charge-selective channels in the paracellular pathway between epithelial cells. Am. J. Physiol. Cell. Physiol. **283:**C142–C147.
13. **Coyne, C. B., T. M. Gambling, R. C. Boucher, J. L. Carson, and L. G. Johnson.** 2003. Role of claudin interactions in airway tight junctional permeability. Am. J. Physiol. Lung Cell. Mol. Physiol. **285:**L1166–L1178.
14. **Dallasta, L. M., L. A. Pisarov, J. E. Esplen, J. V. Werley, A. V. Moses, J. A. Nelson, and C. L. Achim.** 1999. Blood-brain barrier tight junction disruption in human immunodeficiency virus-1 encephalitis. Am. J. Pathol. **155:**1915–1927.
15. **Davson, H., and M. B. Segal.** 1996. Physiology of the CSF and blood-brain barrier. CRC Press, New York, N.Y.
16. **Dermietzel, R.** 1975. Junctions in the central nervous system of the cat. V. The junctional complex of the pia-arachnoid membrane. Cell Tissue Res. **164:**309–329.
17. **Fanning, A. S., B. J. Jameson, L. A. Jesaitis, and J. M. Anderson.** 1998. The tight junction protein ZO-1 establishes a link between the transmembrane protein occludin and the actin cytoskeleton. J. Biol. Chem. **273:**29745–29753.
18. **Furuse, M., K. Furuse, H. Sasaki, and S. Tsukita.** 2001. Conversion of zonulae occludentes from tight to leaky strand type by introducing claudin-2 into Madin-Darby canine kidney I cells. J. Cell Biol. **153:**263–272.
19. **Furuse, M., H. Sasaki, K. Fujimoto, and S. Tsukita.** 1998. A single gene product, claudin-1 or -2, reconstitutes tight junction strands and recruits occludin in fibroblasts. J. Cell Biol. **143:**391–401.
20. **Furuse, M., H. Sasaki, and S. Tsukita.** 1999. Manner of interaction of heterogeneous claudin species within and between tight junction strands. J. Cell Biol. **147:**891–903.
21. **Giles, N. M., A. B. Watts, G. I. Giles, F. H. Fry, J. A. Littlechild, and C. Jacob.** 2003. Metal and redox modulation of cysteine protein function. Chem. Biol. **10:**677–693.
22. **Gonzalez-Mariscal, L., B. Chavez de Ramirez, A. Lazaro, and M. Cereijido.** 1989. Establishment of tight junctions between cells from different animal species and different sealing capacities. J. Membr. Biol. **107:**43–56.
23. **Guo, P., A. M. Weinstein, and S. Weinbaum.** 2003. A dual-pathway ultrastructural model for the tight junction of rat proximal tubule epithelium. Am. J. Physiol. Renal Physiol. **285:**F241–F257.
24. **Haskins, J., L. Gu, E. S. Wittchen, J. Hibbard, and B. R. Stevenson.** 1998. ZO-3, a novel member of the MAGUK protein family found at the tight junction, interacts with ZO-1 and occludin. J. Cell Biol. **141:**199–208.
25. **Hisatome, I., Y. Kurata, N. Sasaki, T. Morisaki, H. Morisaki, Y. Tanaka, T. Urashima, T. Yatsuhashi, M. Tsuboi, F. Kitamura, J. Miake, S. Takeda, S. Taniguchi, K. Ogino, O. Igawa, A. Yoshida, R. Sato, N. Makita, and C. Shigemasa.** 2000. Block of sodium channels by divalent mercury: role of specific cysteinyl residues in the P-loop region. Biophys. J. **79:**1336–1345.
26. **Howarth, A. G., and B. R. Stevenson.** 1995. Molecular environment of ZO-1 in epithelial and non-epithelial cells. Cell Motil. Cytoskeleton **31:**323–332.
27. **Hua, V. B., A. B. Chang, J. H. Tchieu, N. M. Kumar, P. A. Nielsen, and M. H. Saier, Jr.** 2003. Sequence and phylogenetic analyses of 4 TMS junctional proteins of animals: connexins, innexins, claudins and occludins. J. Membr. Biol. **194:**59–76.
28. **Inai, T., J. Kobayashi, and Y. Shibata.** 1999. Claudin-1 contributes to the epithelial barrier function in MDCK cells. Eur. J. Cell Biol. **78:**849–855.
29. **Itoh, M., M. Furuse, K. Morita, K. Kubota, M. Saitou, and S. Tsukita.** 1999. Direct binding of three tight junction-associated MAGUKs, ZO-1, ZO-2, and ZO-3, with the COOH termini of claudins. J. Cell Biol. **147:**1351–1363.
30. **Jonas, C. R., T. R. Ziegler, L. H. Gu, and D. P. Jones.** 2002. Extracellular thiol/disulfide redox state affects proliferation rate in a human colon carcinoma (Caco2) cell line. Free Radic. Biol. Med. **33:**1499–1506.
31. **Kiuchi-Saishin, Y., S. Gotoh, M. Furuse, A. Takasuga, Y. Tano, and S. Tsukita.** 2002. Differential expression patterns of claudins, tight junction membrane proteins, in mouse nephron segments. J. Am. Soc. Nephrol. **13:**875–886.
32. **Kojima, S., C. Rahner, S. Peng, and L. J. Rizzolo.** 2002. Claudin 5 is transiently expressed during the development of the retinal pigment epithelium. J. Membr. Biol. **186:**81–88.
33. **Lesage, F., R. Reyes, M. Fink, F. Duprat, E. Guillemare, and M. Lazdunski.** 1996. Dimerization of TWIK-1 K+ channel subunits via a disulfide bridge. EMBO J. **15:**6400–6407.
34. **Liebner, S., U. Kniesel, H. Kalbacher, and H. Wolburg.** 2000. Correlation of tight junction morphology with the expression of tight junction proteins in blood-brain barrier endothelial cells. Eur. J. Cell Biol. **79:**707–717.
35. **Lippoldt, A., S. Liebner, B. Andbjer, H. Kalbacher, H. Wolburg, H. Haller, and K. Fuxe.** 2000. Organization of choroid plexus epithelial and endothelial cell tight junctions and regulation of claudin-1, -2 and -5 expression by protein kinase C. Neuroreport **11:**1427–1431.
36. **Madara, J. L.** 1998. Regulation of the movement of solutes across tight junctions. Annu. Rev. Physiol. **60:**143–159.
37. **Mark, K. S., and T. P. Davis.** 2002. Cerebral microvascular changes in permeability and tight junctions induced by hypoxia-reoxygenation. Am. J. Physiol. Heart Circ. Physiol. **282:**H1485–H494.
38. **McCarthy, K. M., S. A. Francis, J. M. McCormack, J. Lai, R. A. Rogers, I. B. Skare, R. D. Lynch, and E. E. Schneeberger.** 2000. Inducible expression of claudin-1-myc but not occludin-VSV-G results in aberrant tight junction strand formation in MDCK cells. J. Cell Sci. **113:**3387–3398.
39. **Mitic, L., V. Unger, and J. M. Anderson.** 2003. Expression, solubilization, and biochemical characterization of the tight junction transmembrane protein claudin-4. Protein Sci. **12:**218–227.
40. **Miyamori, H., T. Takino, Y. Kobayashi, H. Tokai, Y. Itoh, M. Seiki, and H. Sato.** 2001. Claudin promotes activation of pro-matrix metalloproteinase-2 mediated by membrane-type matrix metalloproteinases. J. Biol. Chem. **276:**28204–28211.
41. **Morita, K., H. Sasaki, M. Furuse, and S. Tsukita.** 1999. Endothelial claudin: claudin-5/TMVCF constitutes tight junction strands in endothelial cells. J. Cell Biol. **147:**185–194.
42. **Nasdala, I., K. Wolburg-Buchholz, H. Wolburg, A. Kuhn, K. Ebnet, G. Brachtendorf, U. Samulowitz, B. Kuster, B. Engelhardt, D. Vestweber, and S. Butz.** 2002. A transmembrane tight junction protein selectively expressed on endothelial cells and platelets. J. Biol. Chem. **277:**16294–16303.
43. **Nitta, T., M. Hata, S. Gottoh, Y. Seo, H. Sasaki, N. Hashimoto, M. Furuse, and S. Tsukita.** 2003. Size-selective loosening of the blood-brain barrier in claudin-5-deficient mice. J. Cell Biol. **161:**653–660.
44. **Poliak, S., S. Matlis, C. Ullmer, S. S. Scherer, and E. Peles.** 2002. Distinct claudins and associated PDZ proteins form different autotypic tight junctions in myelinating Schwann cells. J. Cell Biol. **159:**361–372.
45. **Rahner, C., L. L. Mitic, and J. M. Anderson.** 2001. Heterogeneity in expres-

sion and subcellular localization of claudins 2, 3, 4, and 5 in the rat liver, pancreas, and gut. Gastroenterology **120:**411–422.
46. **Regina, A., F. Roux, and P. A. Revest.** 1997. Glucose transport in immortalized rat brain capillary endothelial cells in vitro: transport activity and GLUT1 expression. Biochim. Biophys. Acta **1335:**135–143.
47. **Reuss, L., B. Simon, and C. U. Cotton.** 1992. Pseudo-streaming potentials in Necturus gallbladder epithelium. II. The mechanism is a junctional diffusion potential. J. Gen. Physiol. **99:**317–338.
48. **Saitou, M., M. Furuse, H. Sasaki, J. D. Schulzke, M. Fromm, H. Takano, T. Noda, and S. Tsukita.** 2000. Complex phenotype of mice lacking occludin, a component of tight junction strands. Mol. Biol. Cell **11:**4131–4142.
49. **Sasaki, H., C. Matsui, K. Furuse, Y. Mimori-Kiyosue, M. Furuse, and S. Tsukita.** 2003. Dynamic behavior of paired claudin strands within apposing plasma membranes. Proc. Natl. Acad. Sci. USA **100:**3971–3976.
50. **Saunders, N. R., G. W. Knott, and K. M. Dziegielewska.** 2000. Barriers in the immature brain. Cell. Mol. Neurobiol. **20:**29–40.
51. **Staehelin, L. A.** 1973. Further observations on the fine structure of freeze-cleaved tight junctions. J. Cell Sci. **13:**763–786.
52. **Tsukita, S., and M. Furuse.** 2000. Pores in the wall: claudins constitute tight junction strands containing aqueous pores. J. Cell Biol. **149:**13–16.
53. **Van der Goes, A., D. Wouters, S. M. Van Der Pol, R. Huizinga, E. Ronken, P. Adamson, J. Greenwood, C. D. Dijkstra, and H. E. De Vries.** 2001. Reactive oxygen species enhance the migration of monocytes across the blood-brain barrier in vitro. FASEB J. **15:**1852–1854.
54. **Van Itallie, C., C. Rahner, and J. M. Anderson.** 2001. Regulated expression of claudin-4 decreases paracellular conductance through a selective decrease in sodium permeability. J. Clin. Investig. **107:**1319–1327.
55. **van Os, C. H., M. D. de Jong, and J. F. Slegers.** 1974. Dimensions of polar pathways through rabbit gallbladder epithelium. The effect of phloretin on nonelectrolyte permeability. J. Membr. Biol. **15:**363–382.
56. **Wang, F., B. Daugherty, L. L. Keise, Z. Wei, J. P. Foley, R. C. Savani, and M. Koval.** 2003. Heterogeneity of claudin expression by alveolar epithelial cells. Am. J. Respir. Cell. Mol. Biol. **29:**62–70.
57. **Wang, W., W. L. Dentler, and R. T. Borchardt.** 2001. VEGF increases BMEC monolayer permeability by affecting occludin expression and tight junction assembly. Am. J. Physiol. Heart Circ. Physiol. **280:**H434–H440.
58. **Wen, H., E. A. Nagelhus, M. Amiry-Moghaddam, P. Agre, O. P. Ottersen, and S. Nielsen.** 1999. Ontogeny of water transport in rat brain: postnatal expression of the aquaporin-4 water channel. Eur. J. Neurosci. **11:**935–945.
59. **Yu, A. S., A. H. Enck, W. I. Lencer, and E. E. Schneeberger.** 2003. Claudin-8 expression in Madin-Darby canine kidney cells augments the paracellular barrier to cation permeation. J. Biol. Chem. **278:**17350–17359.